

Application of Unmanned Aerial Vehicle Hangar in Transmission Tower Inspection Considering the Risk Probabilities of Steel Towers

ZIFA LIU^{ID}, (Senior Member, IEEE), XINYUE WANG^{ID}, AND YUNYANG LIU^{ID}

School of Electric and Electronic, North China Electric Power University, Beijing 102206, China

Corresponding author: Xinyue Wang (hpawangxinyue@163.com)

ABSTRACT As a typical Internet of Things (IoT) application of the transmission grid, Unmanned Aerial Vehicle (UAV) is the most feasible solution to replace conventional human maintenance resources during the inspection of power transmission lines. However, limited by the flying range and endurance time, it cannot realize the goal of full-autonomous inspection proposed by the State Grid. Based on the UAV inspection technology and the emerging UAV hangar, a new idea of using smart hangar as a connection point to realize full-autonomous inspection of UAV is proposed in this paper. And then making full use of the smart hangar to solve the battery capacity problem existing in the process of autonomous inspection of UAV. Finally, according to the inspection requirements of transmission towers, the fixed-wing UAV is used for long-distance inspection, and the path planning mathematical model considering the risk probabilities of towers and objective functions is established. Simulation results show that the scheme proposed in this paper can effectively solve the existed problems of UAV inspection.

INDEX TERMS Transmission line inspection, UAV smart hangar, risk probability, fully-autonomous UAV inspection, path planning.

I. INTRODUCTION

With the sustained and rapid development of the national economy, higher and higher requirements for the power industry have been put forward. Due to numerous distribution points and wide coverage of transmission lines, most of them are far away from towns with complex topography and harsh natural environment. Besides, transmission lines and their accessories are exposed to the field for a long time, which will be damaged by mechanical tension, electrical flashover, etc. If these problems cannot be found and repaired in time, it will bring great risks to the stable operation of transmission lines [1]. In order to prevent serious accidents, the operation and maintenance department of the state grid has to invest a lot of manpower, material, and financial resources to inspect the transmission lines every year. At present, the most common inspection method in China is still manual inspection or personally climbing the tower. This inspection method has a series of characteristics: high labor intensity, difficult working conditions, low work efficiency, and difficulty in management. Nowadays, there are more than 2,000 UAVs

in the State Grid in China. Among them, the small multi-rotor UAVs have inspected more than 800,000 towers, and the fixed-wing UAVs inspections have reached more than 90,000 km. More than 380,000 defects have been discovered, and 78.5% of them are located above the upper mouth of the tower, which were difficult to find through manual inspection. In the next three years, the State Grid plans to make a change in inspection mode from manual inspection to human-UAV coordination, finally to fully-autonomous UAV inspection, and comprehensively improve the efficiency of inspection. In the future, the State Grid will realize multi-UAV intelligent collaborative inspection to replace the traditional manual inspection, completing the reform of the inspection mode of power system.

Taking the 10 km line with typical transmission line corridor characteristics (mountains terrain is complex and vegetation cover is dense) in Guizhou province as an example. Table 1 shown below analyzes the difference among manual inspection, traditional remote sensing inspection, and UAV light detection and ranging (LiDAR) inspection in two aspects of social and economic benefits.

With further advancement of power grid construction and transformation, it is necessary to promote the transformation

The associate editor coordinating the review of this manuscript and approving it for publication was Giambattista Grusso^{ID}.

TABLE 1. The difference between manual inspection and UAV inspection.

Social Benefits				
No.	Comparison Program	Manual Inspection	Visible Light Inspection	LiDAR Inspection
1	Flaws of Tower's Accessory	Achievable Inefficiency Low Accuracy	Unachievable	Easily Realization High Efficiency High Accuracy
2	Slope and displacement of tower	Unachievable	cannot detect	Easy Detection
3	Detection of Historical data change	Hard to Achieve	Difficult to Achieve	Easily Realization
4	Digitized inspection results	Unachievable	Achievable	Achievable
Economic Benefits				
No.	Comparison Program	Manual Inspection	Visible Light Inspection	LiDAR Inspection
1	Inspection Time	2-3 Days	30min/1h	30min/1h
2	Human Input	3-4 Person	1 Person	1 Person
3	Unknown factors that Affect the Efficiency of Patrol Inspection	Inspector Injured、Snake Infestation in mountain	No	No

of transmission line inspection from labor-intensive to technology-intensive. The development of mobile robot technology provides a new mobile platform for transmission line inspection, which can replace workers to carry out the inspection. It can also further improve the efficiency and accuracy [2]. The authors of [3] introduced the research status of mobile robots for the transmission lines, and some major efforts to solve the inspection problem are reviewed and discussed. The robots can increase efficiency, reduce labor costs and the risk of injury to maintenance personnel. Although there have been some theoretical research and technological developments in this area, problems related to stability, controllability, and autonomy still exist.

In some countries and regions, route patrol robots and manned helicopter patrol have replaced human patrol. However, due to technical limitations and high costs, it is difficult to fully popularize. UAV is an Unmanned Aerial Vehicle that is operated by radio-controlled equipment or programmed controls. With the rapid development of the aviation industry, science, and technology, the use of UAV for line inspection has become a hot topic in recent years. The great scientific value and application value of the UAV intelligent inspection are gradually reflected. More and more countries

are vigorously developing this business. The University of Wales and its power consulting company in the UK first used UAV to inspect power lines. In 2000, the university and a British technology company successfully carried out the test of high-voltage transmission line inspections with UAV. The result shows that using UAV for line inspection can greatly improve the efficiency, reduce the burden of manual inspection, and timely detect the fault and hidden danger to ensure the normal operation [4]. In 2004, Canadian began to use the UAV-mounted photoelectric pods to carry out high-voltage transmission line inspections, which greatly reduce the cost of inspection. In [5], a novel method is proposed for insulator fault detection, which can detect both one fault and multi-fault in UAV-based aerial images.

The authors of [6] proposed a transmission line inspection system basic framework based on remote sensing. For UAV, safe and continuous autonomous navigation on transmission lines has been a problem. Using the Global Positioning System (GPS) to navigate is a direct and effective method. The authors of [7] developed a quadroter-based detection system that enables autonomous detection of predefined GPS waypoints. Along the transmission corridor, transmission towers are also considered as an important reference for assisting autonomous navigation. For the real-time reliable positioning of transmission towers, a lot of work has been done in [8]–[10]. At present, multi-rotor UAVs have been widely used. [11] briefly describes the advantages of multi-rotor UAV inspection lines, and summarizes the operation process of multi-rotor UAVs.

Path planning is to provide optimal path for drivers, and it is an important part of AI technology, intelligent robot, and intelligent transportation technology [12]. [13] established the path planning mathematical model and objective function according to the task requirements of transmission line corridor inspection and towers inspection, it also considered the performance of multi-rotor UAV. The genetic algorithm is used to solve the path planning of UAV, and the simulation results show that the algorithm adopted in this paper can find the optimal inspection path. Different types of UAVs are suitable for different inspection tasks and have different requirements for path planning. According to the characteristics of the tower monitoring, the multi-rotor UAV is used for the tower inspection in [14]. By considering the safe distance between UAV and the tower and the features of the camera, the genetic algorithm (GA) is used to design a rational inspection path. Then, according to the requirements of the line corridor monitoring mission, the fixed-wing UAV is used for long distance inspection and the path planning mathematical model and objective function are established. The GA and genetic simulated annealing(GSA) algorithms are used to obtain effective inspection paths.

Flying range and endurance time are important parameters for describing the performance of UAVs. Due to the limitation of battery capacity, the duration of UAV is short and the efficiency of inspection is low. Therefore, most research on

the planning of transmission line inspection routes are mainly based on manual or vehicle inspection. [15] established an inspection path planning model for transmission lines based on the vehicle routing problem (VRP). An optimized path to inspect the transmission tower with task requirements was made to optimize the inspection time and the number of required vehicles. Previous studies of transmission line inspection path planning did not take into account the risk probability of the transmission tower, but only with the shortest path or time as an objective function. The authors of [16] improved the transmission line inspection planning model. Bayesian and its reasoning mechanisms are used to classify the risk grades of transmission tower. Under the condition of considering the distance of towers and risk levels of each tower, a multi-objective inspection path planning model is established, and an optimal inspection scheme is formulated. For the problem of flying range and endurance time, the solution of using radio energy transmission in the process of UAV line inspection is proposed by [17].

As mentioned above, the existing problems of UAV inspection are as follows: (1): The autonomy and intelligence level of UAV inspection need to be further improved, which cannot meet the practical inspection requirements. (2): The flying range and endurance time are limited. Each UAV must be equipped with at least 2 inspection personnel, when the power of UAV is insufficient, it should be recovered and replace the battery in time, and then, continue to complete the inspection. In order to realize the goal of transition from manual inspection to man-UAV coordination, and then to fully-autonomous UAV inspection planned by the State Grid in the next three years. Based on the above research, this paper proposes a new idea of using smart hangar as a connection point to realize autonomous inspection of UAV. And then making full use of the emerging smart hangar of UAVs to solve the main problem of the short flying range in UAV autonomous inspections currently existed. Through the interconnection of the smart hangar, the system has the characteristics of one-button take-off and autonomous operation according to the GPS coordinates of the transmission tower compiled in advance. It can also automatic return to the hangar and the image data is uploaded to the control center, which truly realizes the full-autonomous inspection without manual intervention. The full-autonomous inspection solution of UAV for transmission towers is shown in Fig.1.

At the same time, this paper breaks the traditional route planning that only considering the shortest path or the shortest time, but combined with the risk probability of the transmission tower. The priority is given to the transmission tower with high-risk probability while considering the shortest path. The optimal weight ratio of the two is set depends on the actual inspection requirements.

The rest of this paper is organized as follows. In Section 2, the steps of UAV hangar locating is introduced. In Section 3, The risk probability of transmission towers and their computing methods are proposed. The objective function based on risk probability and the shortest path is

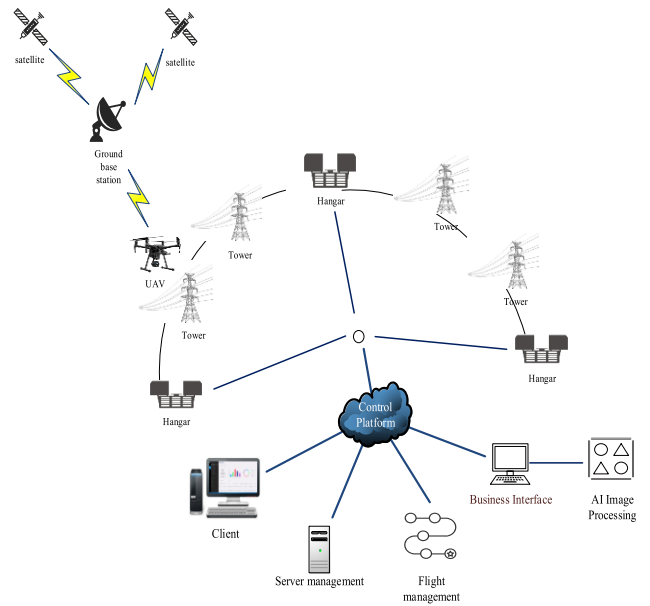


FIGURE 1. UAV intelligent patrol-inspection (UAV-PIS) solution.

established in Section 4, and a case study on routing planning of UAV inspection based on the UAV hangar considering the risk probability of transmission towers is introduced in Section 5.

II. UAV HANGAR LOCATING

According to the inspection experiences and data, the maximum endurance of a domestic brand series multi-rotor UAV can reach 32-38 minutes. The average inspection time of a double loop tower takes 6 minutes, and the average horizontal flight speed is 20 m/s. In order to simplify the calculation, it is approximately considered the battery needs to be replaced every 3 poles inspected. When the endurance time of UAV is less than 6 minutes (this paper describe the UAV's SOC problem as the endurance time to simplify the calculation, here we approximately believe that the power remaining is less than 20%), the UAV needs to find the nearest hangar for battery replacement. It should be noted that it is not necessary to replace the battery after all inspection of towers. Suppose there are 20 poles. The first extreme case is that each hangar will only be visited once (we think that each hangar will be visited at least once), that is, only one battery is used in each hangar, $\text{ceil}((20-3)/3) = 6$. The second extreme case is that each hangar will be visited 3 times, that is, all 4 groups of batteries are used, $\text{ceil}((20-3)/12) = 2$. So the number of hangars is taken as $k = 2, 3, 4, 5, 6$.

step 1: Combining 3 adjacent towers as a group randomly. If there are towers remained after grouping, they are directly regarded as a group. By means of clustering, the groups of towers are regrouping until the distance between 3 towers in each group is shorter than that in other groups. Repeat this step until the distance between the 3 towers in all groups is optimal compared with other cases. Fig. 2(a)-(c) gives a brief grouping process of towers. Here, the center of each

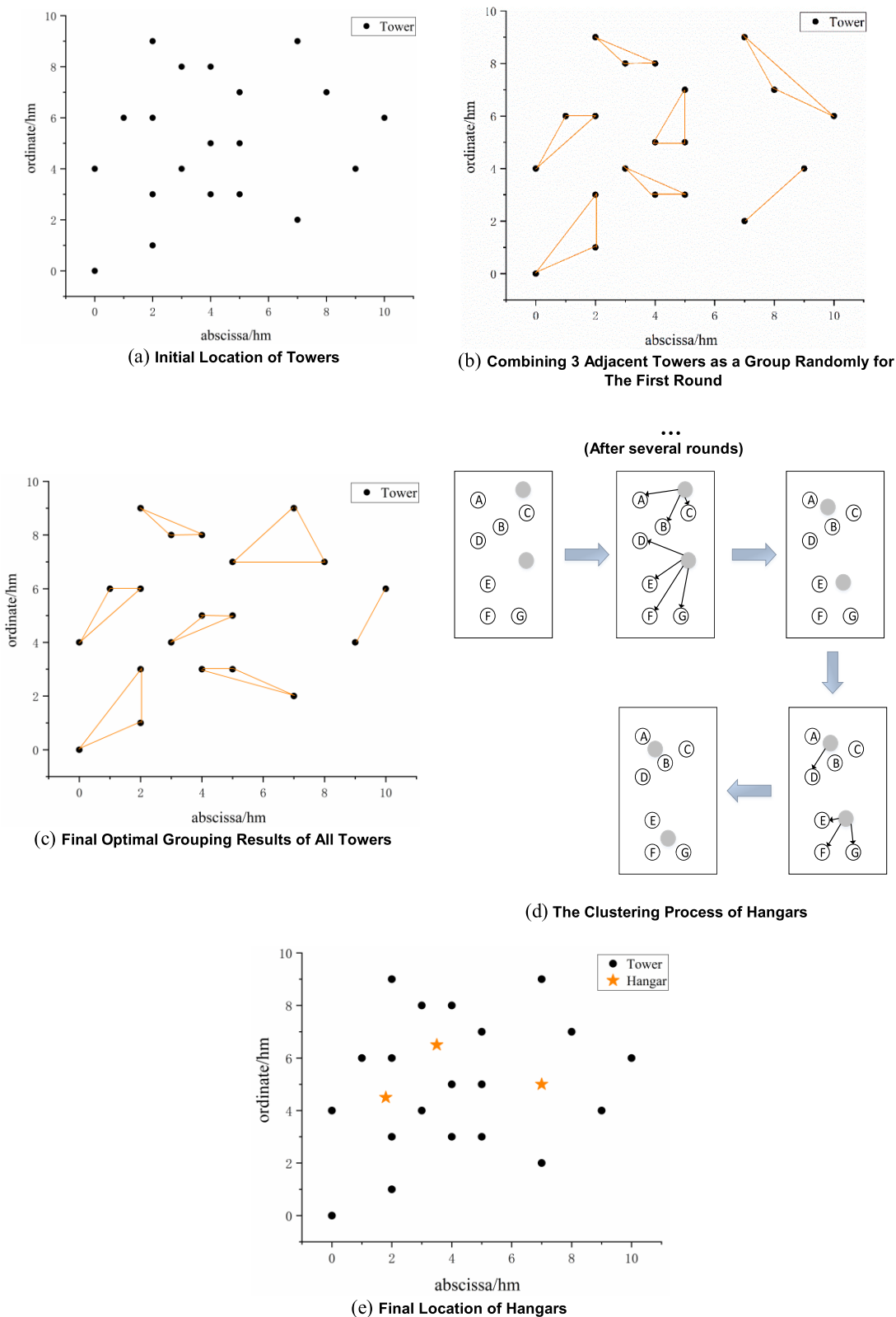


FIGURE 2. Example of location process of 3 hangars.

group is represented by the outer center of the triangle, and the distance to the three vertices of the triangle (tower) is equal.

step 2 (First pass): Take the hangar location as the initial cluster center, assign k records to the initial cluster location randomly. Let $k = 2$ firstly, suppose we specify m_1 and

m_2 randomly, and then to find the nearest cluster center for each group. The Euclidean distances of each group's center points and each cluster's center points m_1, m_2 were recorded. Find the nearest cluster center for each group. The formula for calculating Euclidean distance is $d(C_i, X_j) = \sqrt{(x_i - x_j)^2 + (y_i - y_j)^2}$, where $C_i = \{C_1, C_2\}$ represents the center of cluster, sample set X_j represents the center points of each group.

step 3 (First pass): Find the centroid of each cluster and update the location of each cluster center with the new centroid value. For example, the centroid of cluster 1 is $[(x_1+x_2+x_3)/3, (y_1+y_2+y_3)/3] = (x, y)$, where x_i, y_i represent the center coordinate of each group. At the end of the first pass, the centroid of the cluster has moved.

step 4: Repeat steps 2 and 3 until convergence or termination. Since the centroid has changed, we go back to step 2 and carry out the second work until no cluster center changes compared with the previous processing. The whole clustering location process of 2 hangars is shown in Fig. 2(d).

step 5: Take $k = 3, 4, 5, 6$, and successively to continue the above three steps to get the other four results. For example, the final location of the 3 hangars is shown in Fig. 2(e). Then compare the results with different k values. Take the optimal value under the premise of considering the local geographical environment, the safety redundancy, and the economy. Different areas and situations has different value.

Based on the above steps, Fig.2 gives a general example of set grouping of towers and the clustering process of hangars. The coordinate points shown below are created for the previous work on [15].

III. RISK PROBABILITY OF TRANSMISSION TOWERS

As an important part of the power system, transmission tower is the main support of the power grid, its safe operation is part and parcel for the overall stability of the power system. The transmission tower and its accessories are exposed in the wild all year round. This run mode must be affected by environmental factors, human factors and the equipment itself. Once damaged, it will seriously threaten and destroy the operation of the entire power grid and the safety of the surrounding people. Since the main factors of the risk probability of transmission towers are different in different periods and locations, it is necessary to comprehensively consider the influence of various factors on the operating state of towers in order to quickly and accurately eliminate the potential safety hazards of the towers.

In order to more comprehensively and accurately evaluate the risk probability of transmission towers, several factors that have a significant impact on the operation of transmission towers are selected as the key indicators for assessing the risk of towers. Including the abnormal frequency of transmission tower operation, the slope of the transmission tower location, the distance between the transmission tower and the residential area, the distance from the transmission tower to the river, the inclination of the transmission tower footing, and the

TABLE 2. Initial decision-making table.

IF ₁	IF ₂	IF ₃	...	IF ₆	D
0.5	5	1.2	...	I level	Normal
0.76	10	0.6	...	II level	Abnormal
...
0.69	2	0.9	...	I level	Normal

transmission tower external damage hazard level, etc., where the former are traditional influence factors, and the latter are the risk probability influence factor of the transmission towers considering advanced technology innovation. Based on the advanced BeiDou system and GPS high precision technology, the automatic transmission tower deformation monitoring terminal is developed. Real-time monitoring and early warning are realized for the tower tilted on the subsidence situation. The transmission tower external damage hazard is based on the advanced satellite remote sensing technology, fully exploiting the value of satellite remote sensing image data, quickly identifying typical environmental features around the transmission tower, and monitoring whether it is at a safe distance through multi-temporal remote sensing image change monitoring. It provides powerful decision support for finding the cause of the external force damage of the transmission line in time, such as the newly built industrial park, construction work, etc. The distance between the transmission tower and the river based on the flood identification algorithm. The data of the SAR satellite imagery of the flood with a resolution of 10m is selected to identify the flood fault of the transmission tower.

The influence factors of each transmission tower's risk probability are expressed by IF₁ to IF₆, and D is the decision attribute, that is, the operating state of the tower. In order to construct the original sample sets, the actual operation data must be obtained first. For this reason, some transmission line information, including historical operation information and attribute information in recent years obtained from a regional power bureau, were used to construct the decision table and verify the data. The initial decision table is made as shown in Tab 2.

Part of the data in the table is subject to quantization. The quantification process is to map the characteristics of each influencing factor to a certain interval and express different characteristics with specific values, such as the slope of transmission towers. The Bayesian network model is used to calculate the conditional probability of each attribute in the initial decision table, and then the probabilistic calculation can be used to obtain the high-risk running probability of the sample. There are 372 records in the final decision table, of which 189 are abnormal records, accounting for 50.81% of the total records, and 183 are normal records, accounting for 49.19% of the total records [19].

Where the state variables $B = (B_1, B_2) = (\text{high-risk operation, low-risk operation})$. The high-risk operation probability

of tower is as follows:

$$P_H = P(B_1 | A) = \frac{P(B_1) \prod_{i=1}^6 P(IF_i | B_1)}{P(B_1) \prod_{i=1}^6 P(IF_i | B_1) + P(B_2) \prod_{i=1}^6 P(IF_i | B_1)} \quad (1)$$

where $P(B_1)$, $P(B_2)$ represent the historical high-risk operation probability and low-risk operation probability of the tower, respectively; $P(IF_i | B_1)$ represents the high-risk operation probability of tower under different influencing factors.

Similarly, the low-risk operation probability of this sample is:

$$P_L = P(B_2 | A) = \frac{P(B_2) \prod_{i=1}^6 P(IF_i | B_1)}{P(B_1) \prod_{i=1}^6 P(IF_i | B_1) + P(B_2) \prod_{i=1}^6 P(IF_i | B_1)} \quad (2)$$

IV. ROUTE PLANNING OF UAV INSPECTION CONSIDERING THE RISK PROBABILITY OF TRANSMISSION TOWERS

A. PROBLEM DEFINITION AND MATHEMATICAL MODEL

In the classical TSP model, it is assumed that all nodes just visit once. However, the hangar in this paper sometimes does not need to be visited, and sometimes needs to be visited for several times. So it is difficult to directly use the classical model to solve the UAV inspection problem considering the battery exchange. At the same time, this assumption also makes no subtours in any cases, so all subtours in the classical model need to be eliminated. While it is reasonable to connect one tower to the other tower to form a subtour considering the hangar revisited, the sub-circuit formed between the towers is still not allowed and needs to be eliminated. Therefore, the main improvement of the model is as follows: introduce hangar nodes, district the subtour's type, lose some subtour's constraint and improved it.

The scene is described as follows. The UAV is dispatched by one hangar, prior to inspect the tower with higher risk probability and ensure the shortest path. After all the towers are inspected, it flies back to the nearest hangar and upload images to the background control center. Then do troubleshooting, battery charging, and other work to prepare for the next inspection. During the inspection, when the power of the UAV is low, the UAV will look for a nearby hangar for battery replacement. Here, we ignore the time it takes to replace the battery after arriving at the hangar. After the replacement, the endurance time of the UAV restored to the maximum time (full power state). And the UAV continues to go to the next tower for inspection according to the planning route.

Due to the complexity of the actual situation, relevant assumptions need to be made before the establishment of

the mathematical. Assumptions make about the UAV path planning in this paper are as follows.

- (1). It is assumed that the power consumption of UAV when flying along the transmission line is proportional to the flight distance/time.
- (2). It is assumed that the location of the hangar is known, and the UAV returns to full power state after visiting the hangar.
- (3). It is assumed that the time for the UAV to replace the battery in the hangar is ignored.
- (4). It is assumed that the speed of UAV remains unchanged during the flight.

Based on the above scenarios, the constraints of the model in this paper can be classified into three categories. (1): Node constraint. Tower node is visited only once, while the hangar node is visited no more than 4 times. (2): Route constraint. The UAV starts from one hangar, visits tower and hangar nodes continuously, and finally returns to the nearest hangar after the inspection of the last tower. (3): Battery constraint. The UAV is fully charged only when it leaves the hangar, and the remaining power must ensure that it can reach the next node.

Additional notation used in formulating the UAV-VRP is defined next.

1) SETS

To clarify the model, additional notation used in formulating the UAV-VRP is defined next.

NOMENCLATURE

T	set of towers indexed by t
H	set of hangars indexed by h
V	nodes set indexed by v, $V = TUH$
W	set that determines the existence of subtour is the sum set of sets T' and H', where T' is the true subset of T after removing the empty set, and H' is the set of H.

2) NON-DECISION VARIABLES AND PARAMETERS

NOMENCLATURE

d_{gk}	the distance from node g to node k
t_s^i	the time takes for UAV to inspect the ith tower
Q	UAV's battery capacity
r	the battery consumption rate per unit time
S_v^1	the remaining power when UAV reaches g, $v \in V$
S_v^2	the remaining power when UAV leaves g, $v \in V$

3) DECISION VARIABLE

$$x_{gh} = \begin{cases} 1 & \text{UAV from point g to h} \\ 0 & \text{other} \end{cases}$$

The mathematical formulation of the UAV-VRP is as follows:

$$\min f = \alpha \sum_{i \in V} \sum_{j \in V, g \neq k} x_{ij} d_{ij} + \beta \sum_{i \in T} P_{i+1}/P_i \quad (3)$$

$$\begin{aligned}
 \text{s.t. } & \sum_{v \in V, v \neq t} x_{vt} = 1 \quad \forall t \in T \quad (4) \\
 & \sum_{g \in W} \max_{k \in W} x_{gk} \leq |W| - 1 \\
 & W = T' \cup N', \quad \forall N' \subseteq N, \quad \forall T' \subseteq T, \quad |T'| \geq 1 \quad (5) \\
 & S_k^1 \leq S_f^2 - r \cdot t_{fk} \cdot x_{fk} + Q(1 - x_{fk}) \quad \forall k, f \in V \quad (6) \\
 & S_h^2 = Q \quad \forall h \in H \quad (7) \\
 & S_t^2 = S_t^1 + q \quad \forall t \in T \quad (8) \\
 & \sum_{v \in V, v \neq t} x_{tv} \leq 4 \quad \forall h \in H \quad (9) \\
 & x_{gk} \in \{0, 1\}, \quad \forall g, k \in V \quad (10)
 \end{aligned}$$

The objective function (3) seeks to minimize the sum of total distance and total risk probability, where P_i, P_{i+1} represent the risk probability of transmission tower i and $i + 1$, α, β represent the weighting coefficient. When we require priority to ensure the shortest path, we will increase the proportion of α , and if we require priority to consider the risk probability, we will increase the proportion of β . Constraints (4) ensure that each tower node has exactly one successor: a tower or a hangar. Constraints (5) are improved subtour elimination constraints. The first improvement is the set W , which is used to determine the existence of subtour, is the sum of set T' and N' . Where T' is the true subset of T , N' is the true subset of N . The other improvement is to use $\max_{k \in S} x_{gk}$ to replace $\sum_{h \in S} x_{gh}$ in the classical model, so as to ensure that the result remains 1 even if the hangar is revisited many times. The hangar nodes are introduced into the TSP model through constraints (5), so that the form can be maintained consistent with the classical TSP model without the hangar node, and it is not compulsory that the hangar node must be visited. Constraints (6) track UAV's power level, indicating the relationship between the power of the preceding node and the following node. If the UAV is from f to k , the remaining power when it reaches k is the remaining power when leaving f minus the amount of power consumed on the route from f to k . If the UAV does not go from k to f , Q is the maximum power, which suggests that the constraint is always satisfied, and this constraint is relaxed. Constraints (7) reset the power level to Q upon arrival at the hangar nodes. Constraints (8) indicates that the remaining power when the UAV leaves the tower is the remaining power when it reaches the tower plus the amount of power consumed by the inspection process in this tower. Constraints (9) indicates that the departure times of UAV from the hangar node are no more than 4 times. Constraints (8) defines the decision variable as a 0-1 variable.

The model established above is called a basic model. Although the hangar nodes were introduced by constraints (7) to solve the UAV-TSP problem, the subtour was not distinguished, and the subtour generated by the revisited was still limited by $|W| - 1$. In addition, S_v^1 and S_v^2 cannot identify the specified position of node v in the route, so constraints (6) only take effect for each node at most once, which prevents the revisit process. The existing research to solve the revisit

problem is to add a ‘‘virtual copy point’’ to each revisit point in the basic model. For example, it is estimated that revisit is at most once, let $H' = H \cup H$, H is replaced by H' . Although this method can partially meet the optimization requirements and does not require major changes to the model, it is necessary to estimate the upper limit of revisit times. Otherwise, the optimal solution may be lost, and multiple solutions may be generated, that is, the same solution is divided into two solutions. In this paper, an extended model is developed to solve the revisit problem. In this model, two non-decision variables S_v^1 and S_v^2 are redefined, so that it can character the previous node in the path, and the power on the node can be constrained for several times.

NOMENCLATURE

- S_{gk}^1 the remaining power when UAV reaches k from g to $k, g, k \in V$
- S_{kf}^2 the remaining power when UAV from k to f leaves $f, k, f \in V$

The other symbols are consistent with the basic model. The whole mathematic model of the extended scenario is presented below:

$$\begin{aligned}
 & \text{Minimize: (1)} \\
 & \text{s.t. (4), (9), (10)} \\
 & \sum_{g \in W} \max_{h \in W} x_{gh} \leq |W| \times \max_{h \in H'} \\
 & \times \left(\sum_{v \in V} x_{vh} - \sum_{v \in S} x_{vh} + 1 \right) - 1 \quad W = T' \cup H' \quad (5') \\
 & S_{gk}^1 \leq S_{fg}^2 - r \cdot t_{gk} \cdot x_{gk} + Q(2 - x_{fg} - x_{gk}) \quad \forall g, k, f \in V \quad (6') \\
 & S_{vn}^2 = Q \quad \forall v \in V, n \in N \quad (7') \\
 & S_{vt}^2 = S_{vt}^1 + q \quad \forall v \in V, t \in T \quad (8')
 \end{aligned}$$

where the objective function (3), constraints (4), (9) and (10) remain unchanged. Constraints (5)-(8) are adjusted to (5')-(8'). Constraints (5') is a further improved subtour constraint, which explain in 4.2. Constraints (6') introduces a relaxation condition more than constraint (6), assuming there are three points g, k and f , only when UAV goes from f to g and then to k , the constraint is meaningful, otherwise the constraint is always true. Constraints (7') and (8') have exactly the same meaning as the corresponding constraints in the basic model, expect that the subscripts of variables are adjusted.

B. REVISIT STRATEGY

Since the hangar node has been introduced in constraint (5), the understanding of constraint (5') is highlighted with its solution to revisit. According to different situations, it can be divided into two types of revisit cases.

Situation 1: All the hangar in the selected subtour are only visited once, that is there is no revisit. At this time, no subtour

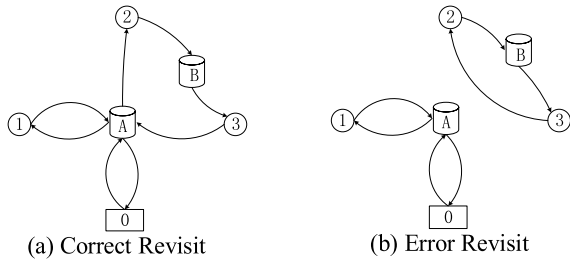


FIGURE 3. Revisit examples.

TABLE 3. The data of 20-steel tower transmission network.

Param.	No.									
	1	2	3	4	5	6	7	8	9	10
X (hm)	5	3	0	2	0	7	1	8	4	9
Y (hm)	5	4	0	3	4	2	6	7	3	4
P_i	0.97	0.9	0.88	0.99	0.79	0.82	0.85	0.7	0.77	0.72

Param.	No.									
	11	12	13	14	15	16	17	18	19	20
X (hm)	7	2	10	3	5	2	5	4	2	2
Y (hm)	9	1	6	8	7	6	3	8	9	5
P_i	0.69	0.65	0.61	0.62	0.61	0.8	0.76	0.89	0.76	0.89

is allowed to form between the tower nodes, and the subtour cannot be generated.

Now, $\sum_{v \in V} x_{vh} = \sum_{v \in S} x_{vh}$, which equivalent to $\sum_{g \in S} \max_{h \in S} x_{gh} \leq |S| - 1$.

In Fig.3(a), since the hangar B is only visited once, the subpath -2-B-3- fits the situation 1. Fig.3(b) is against situation 1, that is the subpath -2-B-3-2 is formed. Since the hangar existing in this loop does not reenter, the subtour cannot be formed.

Situation 2: If there is a revisit of the hangar in the subtour, but this revisit is not completely included in the subpath, that is, this part of the tower can be connected to other nodes by revisiting a hangar, then the subpath may have a subtour.

Now, $\sum_{v \in V} x_{vh} > \sum_{v \in S} x_{vh}$, $\sum_{v \in V} x_{vh} - \sum_{v \in S} x_{vh} + 1 > 1$, constraint is always established.

In Fig.3(a), when considering the subpath -A-2-B-3-, although hangar A has to revisit, it also has revisited in the other subpath -A-1-, that is, the original subpath does not contain all revisit situations (0-A-1-A-2-B-3-A-0 or 0-A-2-B-3-A-1-A-0). Therefore, it fits the situation 2.

V. CASE STUDY

The 20 sets of tower data used in this case are coming from the previous work on [18]. Table 3 includes tower coordinates and the risk probability of each tower, the latter is calculated by the risk probability factor data of each tower and formulas in Section 3. The locations of the hangar were selected according to the distribution of 20 groups of towers, each hangar’s coordinates can be obtained based on the content in section 2 as shown in Table 4.

TABLE 4. The data of 3-hangar.

Param.	No.		
	1	2	3
X (hm)	1.8	3.5	7
Y (hm)	4.5	6.5	5

TABLE 5. The optimal solutions with different weights.

α	β	Optimal Path	$\min f$
0	1	I → 4 → 1 → 2 → 20 → II → 6 → 9 → 19 → II → 17 → 16 → 7 → 18 → II → 3 → 5 → 10 → III → 8 → 1 → 12 → 14 → II → 15 → 13 → III	1.0012
0.1	0.9	I → 4 → 3 → 12 → 6 → III → 11 → 8 → 13 → 10 → III → 1 → 17 → 9 → 2 → I → 5 → 7 → 16 → 20 → II → 18 → 19 → 14 → 15 → II	1.0127
0.2	0.8	I → 4 → 12 → 3 → 5 → I → 16 → 20 → 1 → 2 → I → 7 → 19 → 14 → 18 → II → 11 → 8 → 13 → 10 → III → 6 → 17 → 9 → 15 → II	1.0083
0.3	0.7	I → 4 → 2 → 9 → 17 → III → 6 → 12 → 3 → 5 → I → 7 → 19 → 14 → 18 → II → 16 → 20 → 1 → 15 → II → 11 → 8 → 13 → 10 → III	1.0110
0.4	0.6	I → 16 → 14 → 19 → 7 → I → 4 → 12 → 3 → 5 → I → 2 → 9 → 17 → 6 → III → 10 → 13 → 8 → 11 → III → 1 → 20 → 18 → 15 → II	1.0055
0.5	0.5	I → 4 → 12 → 3 → 5 → I → 7 → 16 → 19 → 14 → II → 18 → 1 → 20 → 2 → I → 9 → 17 → 6 → 10 → III → 13 → 8 → 11 → 15 → II	0.99287
0.6	0.4	I → 7 → 5 → 3 → 12 → I → 16 → 20 → 15 → 18 → II → 1 → 17 → 9 → 4 → I → 2 → 6 → 10 → 13 → III → 8 → 11 → 19 → 14 → II	1.0098
0.7	0.3	I → 7 → 5 → 3 → 12 → I → 2 → 20 → 1 → 15 → II → 18 → 14 → 19 → 16 → I → 4 → 9 → 17 → 6 → III → 10 → 13 → 8 → 11 → III	0.98974
0.8	0.2	I → 2 → 9 → 17 → 1 → III → 6 → 12 → 3 → 4 → I → 5 → 7 → 16 → 20 → II → 11 → 8 → 13 → 10 → III → 15 → 18 → 19 → 14 → II	0.96419
0.9	0.1	I → 4 → 12 → 3 → 5 → I → 2 → 9 → 17 → 6 → III → 10 → 13 → 8 → 11 → III → 15 → 18 → 19 → 14 → II → 1 → 20 → 16 → 7 → I	0.9638
1	0	I → 7 → 16 → 2 → 4 → I → 5 → 3 → 12 → 17 → III → 6 → 10 → 13 → 8 → III → 11 → 18 → 19 → 14 → II → 15 → 1 → 20 → 9 → I	0.95417

The improved ant colony algorithm is used in this paper. In the traditional ant colony algorithm, the heuristic function in the search rule considers only the length of the next path, that is, the heuristic function is the reciprocal of the distance between two points, $\eta_{ij} = \frac{1}{d_{ij}}$, the shorter the distance, the greater the value of the heuristic function. On this basis, this paper improves the heuristic function, and the formula representing the risk probability is added to the numerator, $\eta_{ij} = \frac{P_j/P_i}{d_{ij}}$, where d is the distance between tower i and j , P_i is the risk probability of transmission tower, which is calculated by the Bayesian network model in section 3. Therefore, the expectation of each path not only considers its length, but also considers the content contained in the objective function simultaneously, namely risk probability, thus meets our requirements. The first is to ensure the shortest inspection distance, that is, to complete the inspection task as soon as possible. The second is to ensure that the transmission tower with higher risk probability should be dealt with as early as possible.

The experiments were run on a desktop with Intel(R) Core(TM) i5-3230M CPU, 64-bit platform with 2.60 GHz

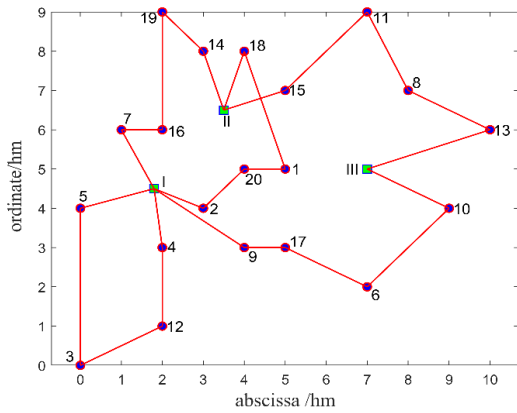


FIGURE 4. Inspection path when $\alpha = 0.5$, $\beta = 0.5$.

TABLE 6. Comparison of several algorithm on inspection paths.

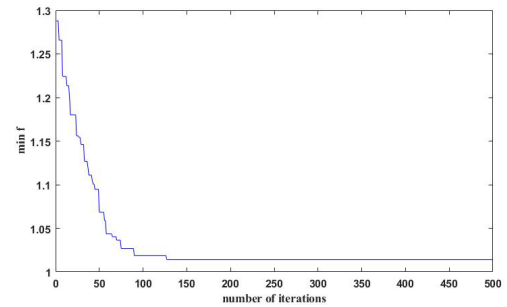
Algorithm	Optimal Path	min f
ACO	I → 16 → 14 → 19 → 7 → I → 4 → 12 → 3 → 5 → I → 2 → 9 → 17 → 6 → III → 10 → 13 → 8 → 11 → III → 1 → 20 → 18 → 15 → II	1.0142
PSO	I → 7 → 5 → 3 → 12 → I → 16 → 20 → 15 → 18 → II → 1 → 17 → 9 → 4 → I → 2 → 6 → 10 → 13 → III → 8 → 11 → 19 → 14 → II	1.0364
GA	I → 4 → 2 → 9 → 1 → III → 6 → 10 → 13 → 8 → III → 17 → 12 → 3 → 5 → I → 16 → 7 → 19 → 14 → II → 20 → 18 → 11 → 15 → II	1.0282
Improved ACO	I → 4 → 2 → 9 → 1 → III → 6 → 10 → 13 → 8 → III → 17 → 12 → 3 → 5 → I → 16 → 7 → 19 → 14 → II → 20 → 18 → 11 → 15 → II	0.96334

processor and 8.00 GB of RAM. The optimization results of the inspection using the improved ant colony algorithm under different weights are shown in Table 5.

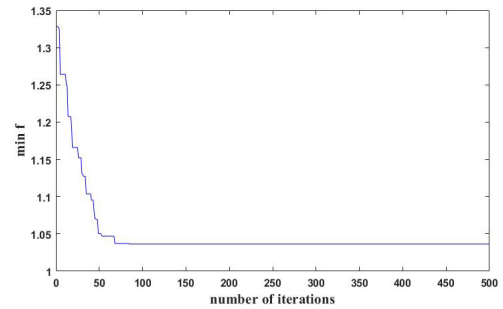
The weight coefficients x and y in the objective function corresponding to the importance of each sub-objective function in this problem, which can be interpreted as the importance of this target relative to the other target, reflecting the intention of the decision-maker, namely the power system’s inspector. In this way, we can meet the requirements of different inspection contents in different periods by adjusting the weight coefficient. For example, daily inspections are mainly for the routine examination for materials in the upper part of the tower, insulators and ancillary facilities. We can set a larger value of the weight coefficient. Besides, special inspection such as seasonal inspection and targeted inspection are mainly based on seasonal characteristics, internal and external surroundings of equipment, and special production needs. These special inspections include forest fire inspection, external force damage inspection, and post-disaster inspection, etc. In this condition, the value of the weight coefficient can be set larger.

One of the inspection paths, which set in Table 5 is shown in Fig.4.

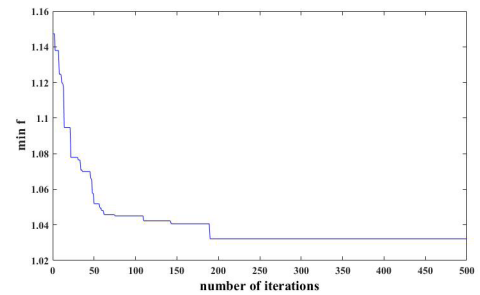
According to the data of transmission towers and hangars provided in Table 3 and 4, the original ant colony optimization



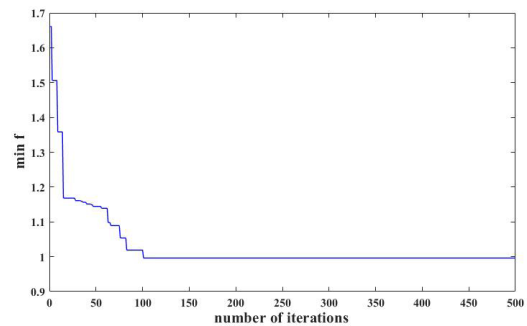
(a) ACO



(b) PSO



(c) GA



(d) Improved ACO

FIGURE 5. Optimization results and number of iterations between different algorithm.

(ACO), the genetic algorithm (GA), and the particle swarm optimization (PSO) were used respectively to compare. The parameters of the original ACO are set as follows: population size 100, number of iterations 500, crossover probability 0.8, generation gap 0.9 and mutation probability 0.2. PSO algorithm parameters are set population size 100, number of iterations 1000, search space 20%, inertia weight 0.6. The parameters of the GA algorithm are set as follows: population

size 100, evolutionary algebra 1000, crossover probability 0.7 and mutation probability 0.005. The obtained inspection path and the value of objective function are shown in Table 6.

The optimization results and number of iterations of the comparison between different algorithm are displayed, as shown in Fig.5, from where we can come to a conclusion that the improved ACO algorithm proposed in this paper is significantly better than the other three algorithms, indicating that the improved ACO algorithm is effective for the optimization of transmission line inspection path.

VI. CONCLUSION

In this paper, the study focuses on providing an automated way for UAV's inspection at the electricity distribution network, which will help with the network maintenance, especially in areas that are not easily accessible by inspectors. The key concept is to improve the traditional TSP problem by using the hangar to connect UAV so that the inspection process can be accomplished fully-autonomous. Besides, this paper introduces the risk probability of transmission towers to break the traditional path planning problem. The inspection path planning was considering the risk probability, which can more comprehensive and targeted to the transmission line inspection path planning.

The ongoing and future work will focus on the optimization of the algorithm and the expansion of UAV's numbers. Besides, it is no longer limited to just one UAV for transmission line inspection, the technology of multi-UAVs cooperation can be applied in this field. In the future, task assignment and path planning are the two core components of the mission planning technology for UAVs.

REFERENCES

- [1] A. Zormpas, K. Moirogiorgou, K. Kalaitzakis, G. A. Plokamakis, P. Partsinevelos, G. Giakos, and M. Zervakis, "Power transmission lines inspection using properly equipped unmanned aerial vehicle (UAV)," in *Proc. IEEE Int. Conf. Imag. Syst. Techn. (IST)*, Krakow, Poland, Oct. 2018, pp. 1–5.
- [2] Z. Yunchu, L. Zize, and T. Min, "Mobile robot for overhead power line inspection—A review," *Robot*, vol. 26, no. 5, pp. 467–473, 2004.
- [3] R. S. Gonçalves and J. C. M. Carvalho, "Review and latest trends in mobile robots used on power transmission lines," *Int. J. Adv. Robot. Syst.*, vol. 10, p. 408, Jan. 2013.
- [4] H. Eisenbeiss, "A mini unmanned aerial vehicle (UAV): System overview and image acquisition," *Remote Sens. Spatial Inf. Sci.*, vol. 36, pp. 1–7, Nov. 2004.
- [5] J. Han, Z. Yang, Q. Zhang, C. Chen, H. Li, S. Lai, G. Hu, C. Xu, H. Xu, D. Wang, and R. Chen, "A method of insulator faults detection in aerial images for high-voltage transmission lines inspection," *Appl. Sci.*, vol. 9, no. 10, pp. 1–22, Oct. 2019.
- [6] X.-Y. Peng, Z.-J. Liu, X.-M. Mai, Z. B. Luo, K. Wang, and X. W. Xie, "A transmission line inspection system based on remote sensing: System and its key technologies," *Remote Sens. Inf.*, vol. 31, no. 1, pp. 51–57, Feb. 2015.
- [7] L. F. Luque-Vega, B. Castillo-Toledo, A. Loukianov, and L. E. Gonzalez-Jimenez, "Power line inspection via an unmanned aerial system based on the quadrotor helicopter," in *Proc. 17th IEEE Medit. Electrotech. Conf. (MELECON)*, Apr. 2014, pp. 393–397.
- [8] C. Sampedro, C. Martinez, A. Chauhan, and P. Campoy, "A supervised approach to electric tower detection and classification for power line inspection," in *Proc. Int. Joint Conf. Neural Netw. (IJCNN)*, Jul. 2014, pp. 1970–1977.
- [9] A. Cerón, I. Mondragón, and F. Prieto, "Real-time transmission tower detection from video based on a feature descriptor," *IET Comput. Vis.*, vol. 11, no. 1, pp. 33–42, Feb. 2017.
- [10] H. J. Zhang and X. S. Zhao, "Design and implementation of the management system of transmission line inspection based on GPS," *Power Syst. Technol.*, vol. 29, no. 7, pp. 78–81, Apr. 2005.
- [11] W. Zheng, F. Zhang, J. Jiao, X. Wang, and H. Chen, "Application of multi-rotor UAV in transmission line inspection," *China Electr. Power (Technol. Ed.)*, vol. 2016, pp. 70–73, Apr. 2016.
- [12] J. S. Gyorfi, D. R. Gamota, S. M. Mok, J. B. Szczech, M. Toloo, and J. Zhang, "Evolutionary path planning with subpath constraints," *IEEE Trans. Electron. Packag. Manuf.*, vol. 33, no. 2, pp. 143–151, Apr. 2010.
- [13] D. Xiong, "The research and application of path planning for UAV inspection transmission line?" M.S. thesis, Dept. Electron. Eng., Wuhan Univ., Wuhan, China, 2014.
- [14] J. Cui, Y. Zhang, S. Ma, Y. Yi, J. Xin, and D. Liu, "Path planning algorithms for power transmission line inspection using unmanned aerial vehicles," in *Proc. 29th Chin. Control Decis. Conf. (CCDC)*, May 2017, pp. 2304–2309.
- [15] Y. Shi, J. Jiang, D. Zheng, Z. Yang, and X. Huang, "Route planning and modeling of transmission lines inspection," *Appl. Sci. Technol.*, vol. 38, no. 11, pp. 18–21, Nov. 2011.
- [16] Y. Q. Ou, J. Z. Wen, and L. G. Wang, "Application of small world based crisscross optimization algorithm in power transmission lines inspection," *Power Syst. Clean Energy*, vol. 32, no. 6, pp. 46–52, Jun. 2016.
- [17] B. Y. Chen and J. Fan, "Exploration of application of UAV in transmission line inspection," *Electr. Eng.*, vol. 3, pp. 80–81 and 85, Mar. 2019.
- [18] M. J. Li, T. J. Gan, and K. Lai, "Power transmission line inspection planning optimization considering risk probabilities of steel towers," *Power Syst. Clean Energy*, vol. 32, no. 10, pp. 61–67 and 78, Oct. 2016.
- [19] Q.-C. Duan and Y.-F. Cheng, "Application of rough set and decision tree theory to inspection of power transmission line," *Comput. Syst. Appl.*, vol. 20, no. 6, pp. 155–160, Jun. 2011.



ZIFA LIU (SM'07) received the B.Sc. and M.Sc. degrees in electrical engineering from Northeast Electric Power University, Jilin, China, in 1995 and 2000, respectively, and the Ph.D. degree from Tianjin University, Tianjin, China, in 2005.

Since 2006, he has been with the North China Electrical Power University, Beijing, China, where he is currently a Professor with the Department of Electrical and Electronic Engineering. He has authored more than 50 technical articles in his research areas and holds ten patents. His research interests include grid planning, renewable energy access to the grid, comprehensive assessment, and distributed generation technology.



XINYUE WANG was born in Anyang, China, in November 1996. She received the B.Sc. degree in automation engineering from Henan Polytechnic University, in 2018. She is currently pursuing the M.Sc. degree with North China Electric Power University.

Her research interests include reconfiguration of distribution networks and intelligent patrol of transmission lines.



YUNYANG LIU was born in Xinji, China, in May 1996. He received the B.Sc. degree in automation engineering from North China Electric Power University, in 2018, where he is currently pursuing the M.Sc. degree.

His research interests include microgrid planning and reconfiguration of distribution networks.

• • •